

# Succinonitrile based solid state electrolytes for dye sensitised solar cells.

*Owen Byrne, Aoife Coughlan, Praveen K. Surolia, K. Ravindranathan Thampi\**

School of Chemical & Bioprocess Engineering, University College Dublin, Belfield, Dublin 4, Ireland

**Abstract:** Succinonitrile (SCN), a solid ion conductor ( $10^{-4}$  -  $10^{-3}$   $\text{Scm}^{-1}$ ) in solid form at room temperature, is mixed with either 1,2-dimethyl-3-propylimidazolium iodide (DMPII) or 1-butyl-3-methyl imidazolium iodide (BMII) ionic liquids for forming a solid plastic phase electrolyte for use in dye sensitised solar cells (DSSC). Cells containing these two electrolytes showed best energy conversion efficiencies of 6.3 % and 5.6 %, respectively. The commonly used DSSC electrolyte additives inhibit the formation of the SCN plastic phase. However, for the first time an SCN-additive (additive = guanidinium thiocyanate) electrolyte composition is reported here, which remains as a solid at room temperatures. Using these new solid electrolytes, a simple and rapid single step filling procedure for making solid state DSSC is outlined. This process, which reduces the required manufacturing steps from four to one, is most suitable for continuous, high-throughput, commercial DSSC manufacturing lines. These new electrolytes have been tested under low incident light levels (200 lx) to investigate their suitability for indoor DSSC applications.

**Keywords:** DSSC, DSC, Dye sensitized solar cell, solid-electrolyte, succinonitrile

\*Correspondence: [ravindranathan.thampi@ucd.ie](mailto:ravindranathan.thampi@ucd.ie).

## 1. Introduction

A typical dye sensitised solar cell (DSSC) consists of a TiO<sub>2</sub> layer electrode chemisorbed with a monolayer of dye molecules to absorb the visible light spectrum. Incoming sunlight is absorbed by the dye generating excited electrons, which are then injected into the conduction band of the TiO<sub>2</sub>. The electrons are routed through an external circuit and a counter electrode to an electrolyte containing a suitable redox species (typically, iodide/tri-iodide couple). The residual oxidized dye cations are instantaneously regenerated by the redox species. Thus the electrolyte is an essential component performing charge transport between the two electrodes and timely dye regeneration as outlined in Figure 1 [1],[2].

The best performing liquid electrolytes to date, achieve >11% efficiency with the iodide/tri-iodide redox couple [3],[4] in acetonitrile/valeronitrile solvents. The present DSSC record of 12.3 % efficiency involves a Co<sup>(II/III)</sup>tris(bipyridyl) tetracyanoborate complex as the redox couple, also in acetonitrile [5]. Recently, water based Co-complex electrolytes have been once again proposed after years of work trying to move away from the traditional water based iodide electrolytes [6]. A major reason for DSSC operational failure in practical applications is due to leakages of liquid electrolyte caused by seal rupture. Liquid based electrolytes not only leak through sealant materials and cause seal failure, but also freeze at low temperatures as to be expected with water and some other solvents. Furthermore, sealant failure can be caused due to the large vapour pressures exerted by volatile organic solvents such as acetonitrile or by the anomalous expansion of H<sub>2</sub>O within the cell. For the advancement of DSSC lifetime guarantee, both these issues need to be resolved. In view of this, various solvent free, gel/quasi-solid and solid state electrolytes have been tested as DSSC electrolytes, including: solvent free eutectic melt of ionic liquids (conversion efficiency,  $\eta = 8.2\%$ ), poly(acrylonitrile-co-vinyl acetate based

gels ( $\eta = 9.03\%$  and  $9.46\%$ ), quasi-solid PVDF based gel ( $\eta = 6.7\%$ ), solid state hole transport materials such as the p-type inorganic hole conductors CsSnI<sub>3</sub> ( $\eta = 3.72\%$ ), copper iodide ( $\eta = 4.7\%$ ) and the organic hole conductor 2,2',7,7'-tetrakis-(N,N-di-p-methoxyphenyl-amine)-9,9'-spirobifluorene (spiro-MeOTAD) ( $\eta = 6\%$ ) and p-type conductive polymers such as poly(3,4-ethylenedioxythiophene) (PEDOT) ( $\eta = 6.1\%$ ) as listed in Table 1 [3-5],[7-16]. Very recently [17], a new record efficiency of  $15.0\%$  was reported by replacing the dye molecule light harvester with an organic–inorganic hybrid perovskite sensitiser (CH<sub>3</sub>NH<sub>3</sub>PbI<sub>3</sub>) coupled with spiro-MeOTAD hole transporter doped with a Co(III) complex as “electrolyte”. However, many of these materials show disadvantages such as the presence of volatile organic solvents [e.g., PVDF and PAN-VA gels], difficult handling conditions, requirement of spin-coating techniques, which involve significant material wastage [e.g., spiro-MeOTAD], extra process steps (additional electrode treatment [e.g., CuI]), and improper pore filling of the mesoporous TiO<sub>2</sub> layers. The fluorine doped CsSnI<sub>2.95</sub>F<sub>0.05</sub> hole conductor mixed with SnF<sub>2</sub> has been reported to achieve  $9.28\%$  efficiency, but the procedure requires both additional pre-treatments of the TiO<sub>2</sub> electrode with fluorine plasma and drying of the cell following infiltration of the solid electrolyte dissolved in an organic solvent. A guaranteed removal of solvent from devices introduces lengthy manufacturing and quality control procedures.

A solid-state material, which solves the problems of electrolyte leakage and seal degradation by highly volatile solvents, is succinonitrile (SCN). SCN is a white-clear plastic crystal possessing characteristics of good conductivity and flexibility. It is a solid at room temperature enabling easy handling under ambient conditions. Plastic crystalline materials such as SCN exhibit rotational disorder, displaying multiple phase transitions, some of which lead to local rotatory motions in the crystal lattice. These rotatory motions cause lattice defect formation,

which are thought to facilitate high molecular/ionic mobility [18]. SCN exhibits a body-centered cubic plastic phase from  $-40^{\circ}\text{C}$  to its melting point at  $58^{\circ}\text{C}$  [19]. In this phase, molecules are rotationally disordered in a mixture of isomers (two gauche isomers and one trans isomer) inverted around the central C-C bond [19]. The availability of the three conformers in succinonitrile creates mono-vacancies in the lattice where the trans isomers act as “impurities” and leads to high molecular diffusivity. It has been shown that plastic crystals mixed with lithium compounds can result in room temperature waxy solids which act as a solid-state solvent or ‘matrix’ for the Li ions exhibiting conductivities as high as  $2 \times 10^{-4} \text{ Scm}^{-1}$  at  $60^{\circ}\text{C}$ , making these materials very attractive for battery applications [20]. SCN is a non-ionic and highly polar plastic-crystalline organic molecule. High polarity enables it to dissolve various types of salts showing ionic conductivity that originates solely from the guest salt in an otherwise non-ionic matrix [21]. Room temperature conductivities up to  $3.4 \times 10^{-4} \text{ Scm}^{-1}$  are obtained with 5 wt.% lithium bis(trifluoromethanesulfonylamide) in SCN [22] and a proton conducting solid electrolyte with conductivities above  $10^{-3} \text{ Scm}^{-1}$  was prepared by incorporating a non-aqueous liquid electrolyte into the plastic crystalline phase of SCN [23]. A series of organic cations containing quaternary ammonium were tested as replacements for metal cations [18]. SCN is reported as a suitable matrix for quaternary ammonium based iodides [tetraethylammonium iodide (TEAI), tetrabutylammonium iodide (TBAI), N-dimethyl, N-propyl, N-butylammonium iodide (DMPBAI), ethyl methyl imidazolium iodide (EMImI), dimethylimidazolium iodide (DMIImI) and ethyl methyl pyrrolidinium iodide (EMPyriI)] and iodine yielding waxy solids in the temperature range  $-40^{\circ}\text{C}$  to  $60^{\circ}\text{C}$ . The resultant materials showed that high  $\text{I}^{-}$  and  $\text{I}_3^{-}$  transport is possible in the solid state with ionic conductivities up to  $3 \times 10^{-3} \text{ Scm}^{-1}$ . The composition of the

electrolyte, both in terms of total iodide/iodine as well as the relative ratio of these has a major effect on the final diffusivities and ionic conductivities [18].

SCN possesses characteristics similar to those that make acetonitrile and glutaronitrile suitable solvents for DSSC [18]. An electrolyte formed by mixing SCN with *N*-methyl-*N*-butyl pyrrolidinium iodide (P<sub>1,4</sub>I) and iodine was reported in DSSC with efficiencies exceeding 6.7 % (at 52 mW/cm<sup>2</sup>), which dropped to approximately 5 % under full sunlight [24]. At 25 °C, this plastic crystal electrolyte has a conductivity of 3.3 x10<sup>-3</sup> Scm<sup>-1</sup>. The DSSC performance of the same electrolyte was recently improved to 6.54 % in full sunlight and 7.93 % at 30 mW/cm<sup>2</sup> using electrospun hierarchically structured TiO<sub>2</sub> nanofiber electrodes [25]. A detailed study employing the same electrolyte (P<sub>1,4</sub>I/I<sub>2</sub>/SCN) also achieved efficiency of 6.54 % under full sunlight using a new two step electrolyte infiltration process, where first the liquid-state electrolyte (E1) containing 0.03M iodine, 0.1M guanidinium thiocyanate, 0.5M 4-*tert*-butylpyridine and 0.6M BMII in acetonitrile:valeronitrile solution (85:15 by volume) was injected into the TiO<sub>2</sub> film and dried at 80°C for 12 h. The high boiling point additives remained entrapped in the TiO<sub>2</sub> pores while most of the solvent was evaporated. After that, the plastic SCN electrolyte was injected into the cell at 80°C. The cell was then cooled to room temperature to obtain a waxy solid electrolyte with the presence of additives showing performance of 6.54 %. Cell performance was further improved by fluorine plasma treatment of the TiO<sub>2</sub> electrode before cell fabrication. This treatment was found to greatly improve infiltration of the SCN electrolyte by increasing the size of nanopores and nanochannels in the TiO<sub>2</sub> electrode and reducing the recombination rate as a result of surface passivation of the TiO<sub>2</sub> nanoparticle surface. Coupled with the two step electrolyte infiltration process, efficiencies of 9.37 % are possible; the best reported for a SCN based solid electrolyte. Addition of 3-D photonic crystals

behind the DSSC to redirect light, not absorbed by the cell in the first pass, back through the active layers improves efficiency to 10.5 %. These additional steps make the cell fabrication procedures lengthy and expensive.

In order for DSSC to compete commercially with other PV technologies, manufacturing line speeds of 2 to >20 m/min are thought to be necessary [26]. Even though, DSSC has become a highly active area of research and development as evidenced by the fast growth of scientific publications and patent applications over the last 15-20 years [27], manufacturing of small laboratory cells is commonly performed by hand without any concern for time or cost optimization. Simple procedures such as dyeing and electrolyte filling are time consuming and at the cell level all steps must be done rapidly and efficiently for producing DSSC modules at commercial scales [28]. Accordingly, industrial processes involving rapid dyeing (for example, in boiling or hot dye baths) are now available to the industry. However, complicated additional steps such as lengthy waiting periods and electrode plasma treatment will again increase DSSC processing times and reduce the cost advantages associated with high speed manufacturing, as envisaged in roll-to-roll manufacturing steps. Prototypes of glass facade elements (70x200 cm<sup>2</sup>) consisting of several serially interconnected DSSC modules each of size 30x30 cm<sup>2</sup> showcased a few typical facade applications of DSSC such as decorative semi-transparent glass panels [29]. Recently, the Fraunhofer Institute for Solar Energy Systems (ISE) developed and fully up scaled a glass frit-sealed DSSC fabrication procedure for manufacturing modules of size 60x100 cm<sup>2</sup> on a single substrate. Cell and panel manufacturing up-scaled to such attractive areas for the building-integrated photovoltaics market is vital for DSSC industrialization [30].

To the best of our knowledge, iodides other than P<sub>1,4</sub>I and LiI have not been reported in SCN based DSSC cells, even though a range of ammonium iodides and imidazolium iodides are

known to show high  $\Gamma$  and  $I_3^-$  transport in solid state matrices [18]. The use of common DSSC electrolyte components such as the imidazolium salts, namely 1,2-dimethyl-3-propyl imidazolium iodide (DMPII) and 1-butyl-3-methyl imidazolium iodide (BMII), in the presence of SCN is another option requiring immediate investigation. Similarly, the effects of common electrolyte additives (TBP, LiI, NMBI, GSCN), which are beneficial to the overall performance of the cell, on the performance of the SCN electrolyte host require clarity.

Therefore, the focus of our current study is threefold:

- Investigate performance of solid SCN electrolytes incorporating iodide salts other than previously reported  $P_{1,4}I$  and LiI.
- Study the effect of common DSSC liquid electrolyte additives (TBP, NMBI, LiI, GSCN) on the performance of solid state SCN electrolytes (open circuit voltage, short circuit current, inhibition of the SCN plastic phase)
- Reduce the required DSSC fabrication steps to allow ready application of SCN based electrolytes in industrial manufacturing process lines.

All electrolyte performances are generally tested under standard 1 sun ( $1000 \text{ W/m}^2$ ), AM1.5 illumination to simulate outdoor conditions. We additionally report here for the first time testing of SCN electrolytes in low, fluorescent light (200 Lx) conditions for applications of solid state DSSC in indoor and sensor device applications. Finally, we propose a quick and simple one step electrolyte filling process ideal for use of these solid electrolytes in high throughput manufacturing process lines.

## 2. Experimental

TiO<sub>2</sub> electrodes were manufactured using the screen-printing method [31], which is based on a layer-by-layer deposition of TiO<sub>2</sub> on a fluorine doped tin oxide (FTO) conducting transparent glass substrate. In all cases, a non-porous dense blocking under-layer of TiO<sub>2</sub> was first deposited on the FTO substrate via TiCl<sub>4</sub> treatment [32] in order to reduce charge recombination. TiO<sub>2</sub> paste was then printed on the TiCl<sub>4</sub> treated glass using a TIFLEX Ltd manual screen-printer and involved several cycles. After each TiO<sub>2</sub> paste deposition, the films were kept in an ethanol chamber for 6 min followed by drying at 125 °C for 6 min, while the final sintering involved gradual heating in an oven at 325°C (5min) followed successively by 375°C (5min), 450°C (15min), and finally at 500°C for 30min. After this sintering step, the electrodes were again treated with TiCl<sub>4</sub> followed by one more sintering at 500°C for 30 mins. The TiO<sub>2</sub> active area was 0.28 cm<sup>2</sup> (consisting of a 6 mm diameter circular spot). The sintered electrodes were placed in a dye bath of N719 [di-tetra butyl ammonium cis-bis(isothiocyanato)bis(2,2'-bipyridyl-4,4'-dicarboxylato)ruthenium(II)] dissolved in acetonitrile:tert-butylalcohol:THF (vol 4.5:4.5:1) for 16-20 hours. Alternatively, a rapid dyeing procedure in hot dye bath is possible as practiced in industries. N719 dye was procured from a commercial supplier (Dyesol Ltd) and used without further purification. The counter electrode was prepared with a thin film of Pt catalyst deposited via a drop of H<sub>2</sub>PtCl<sub>6</sub> solution (2 mg Pt in 1 ml ethanol) and heat treated at 400°C for 15 minutes to remove the solvent. The dye coated TiO<sub>2</sub> electrode and Pt coated counter electrode were sandwiched together and sealed using a Bynel polymer gasket (50 micron thick). Electrolyte was filled into the space between the two electrodes through a hole in the counter electrode via vacuum back filling. The back hole was sealed with a thin piece (0.1 mm thick) of glass, heat sealed with Bynel.

TiO<sub>2</sub> printing pastes employed were a “transparent” paste containing TiO<sub>2</sub> particles of an average size of 20 nm, formed from P25 powder using a standard fabrication procedure [33]. Ethyl cellulose (Fluka, #46080 and #46070) and anhydrous Terpineol (Sigma-Aldrich, 86480) were used as received for making this paste. A “scattering” paste of particle size 150-250 nm was purchased from DyeSol Ltd (WER 2-0). Both pastes were screen printed with a 90 T mesh to yield two electrode configurations used in this study:

- 7+2 (7 transparent layers + 2 scattering layers, total thickness = 15-16 micron)
- 6+0 (6 transparent layers + 0 scattering layers, total thickness = 10 micron)

The optimum reported liquid electrolyte used is labelled E1 and composed of 0.03M iodine, 0.1M guanidinium thiocyanate, 0.5M 4-*tert*-butylpyridine and 0.6M BMII in acetonitrile:valeronitrile solution (85:15 by volume) [33]. SCN based electrolytes were made by heating the SCN host on a hot plate until it becomes a liquid at approximately 80°C. At this temperature the following iodide salts: 1,2-dimethyl-3-propyl imidazolium iodide (DMPII), 1-butyl-3-methyl imidazolium iodide (BMII) and lithium iodide (LiI) were added with stirring. Iodine (I<sub>2</sub>) was then added to yield three solid state compositions in the molar ratio 5:1:100 (X:I<sub>2</sub>:SCN). Electrolytes were vacuum back filled into the DSSC cell in their liquid state at 80°C. The following materials were used as received; 1-butyl-3-methyl imidazolium iodide (BMII, Merck 4.90187.0100), 1,2-dimethyl-3-propylimidazolium iodide (DMPII, Merck 4.94800.0025), guanidinium thiocyanate (GSCN, Merck 8.20613.0250), 4-*tert*-butylpyridine (TBP, Sigma Aldrich 142379-25G), N-methyl benzimidazole (NMBI, Sigma Aldrich 399353-25G), lithium iodide (LiI, Sigma Aldrich 518018-10G), acetonitrile (ACN, Sigma Aldrich 271004-1L), valeronitrile (Sigma Aldrich 155098-100G), succinonitrile (SCN, Sigma Aldrich 160962-25G).

Electro-optical characterization including: current/voltage (I-V) curves, open circuit voltage ( $V_{oc}$ ), short circuit current density ( $J_{sc}$ ) and fill factor (FF), were studied using a *Newport 91195A-1000* solar simulator and *Newport 69920* Arc Lamp Power Supply (**Newport Oriel**, 150 Long Beach Boulevard, Stratford, Connecticut, CT 06615, USA) and recorded with a GAMRY Instruments Potentiostat (**Gamry Instruments**, 734 Louis Drive, Warminster, Pennsylvania, PA 18974, USA). A *Newport 81088A* Air Mass Filter was placed before the output of the solar simulator to simulate AM 1.5 spectrum with irradiance powers of  $1000 \text{ W/m}^2$ . Low intensity I-V curves were also measured with a fluorescent bulb as light source with an illuminance of 200 Lx to simulate indoor lighting conditions.

### 3. Results and discussion

#### 3.1 Succinonitrile based solid electrolytes

The SCN plastic crystal host was infiltrated with DMPII, BMII or LiI and iodine in the molar ratio 5:1:100 (X-I:I<sub>2</sub>:SCN), as described in the experimental section. All three compositions are solid at room temperatures. The performance of these electrolytes was tested in fully fabricated DSSC cells using our 7+2 working electrode configuration. The results from DSSCs fabricated with standard acetonitrile/valeronitrile based liquid electrolyte (E1) is also presented for comparison in Figure 2 and Table 2.

The liquid based electrolyte achieves an efficiency of 8.47 %,  $J_{sc} = 18.1 \text{ mA/cm}^2$  and a particularly attractive  $V_{oc} = 815 \text{ mV}$ . The DSSC formed using the SCN based electrolyte with DMPII showed the best result among the solid electrolytes tested, achieving a best efficiency of 6.33 % [average of four devices,  $\eta = 5.31 \%$  (ESI Table S1)]. This best result compares quite favourably to the P<sub>1,4</sub>I doped SCN performance of 6.54 % [10], exhibiting almost the same  $V_{oc}$

values (707 vs 711 mV), slightly better  $J_{sc}$  (15.6 vs 14.2 mA/cm<sup>2</sup>) but with a lower FF (57 vs 64.7 %). We believe that FF can be improved by rigorous optimization such as introduction of extra process steps, e.g. fluorine plasma treatment of the TiO<sub>2</sub> electrode[10] but our aim in this paper is to keep process steps to a minimum (see Section 3.3). In a large manufacturing line, such additional steps may become practical after appropriate machines and methods are developed.

A solid electrolyte based on BMII was also tested. This is a more suitable comparison to the liquid electrolyte, which also contains the same imidazolium salt. Average performance for four devices was  $\eta = 5.33\%$  (ESI Table S1). Similar shape and fill factor are observed when compared to the liquid electrolyte, but the best performing cell exhibited much reduced  $V_{oc}$  and  $J_{sc}$  values, compared to the liquid E1 electrolyte, resulting in a lower efficiency of 5.62 %. The incident photon to current efficiency (IPCE) spectra of these best performing DMPII and BMII based SCN electrolytes are compared to E1 in ESI, Figure S1. All three show similar shapes with a maximum response of 69 % (E1), 58 % (BMII) and 63 % (DMPII) observed at 525 nm. Much like their J-V curves, the shape of the BMII:I<sub>2</sub>:SCN and BMII containing liquid E1 electrolyte are almost exactly the same (ESI Figure S1(B)), although the IPCE at  $\lambda_{max}$  is much lower for the solid state system, which leads to the observed lower photocurrent. Solid state DMPII:I<sub>2</sub>:SCN, on the other hand, shows slightly lesser IPCE response in the ~350-450 nm region (ESI Figure S1(B)) but its overall greater IPCE contribution compared to BMII:I<sub>2</sub>:SCN leads to the observed larger photocurrent values.

Finally, a LiI based solid electrolyte was also fabricated and efficiencies of 3.58 % were measured. This low performance is due to a significant drop in cell  $V_{oc}$ . The open circuit voltage recorded was 489 mV which is far below the voltages obtained in the reference liquid electrolyte.

The adsorption of the Li cation causes a positive shift in the conduction band energy of the titanium oxide, decreasing Voc [34]. The size of the shift is attributed to the charge-to radius ratio of the cation, i.e. larger counter-cation, larger the open circuit voltages, if the charge remains the same [35],[36]. As lithium ions have a relatively small radius, the open circuit voltage is decreased significantly. Furthermore, the small Li<sup>+</sup> ions can intercalate into the dye sensitised TiO<sub>2</sub> films thereby increasing recombination and further lowering Voc [34]. However, a relatively good performance in Jsc of 14.6 mA/cm<sup>2</sup> is observed.

Previous LiI based SCN electrolytes are reported to achieve an efficiency of 3.92 % in a DSSC with the use of TBP additive (Jsc = 8.76 mA/cm<sup>2</sup>, Voc = 611 mV, FF = 73,  $\eta$  = 3.92 %). However, the TBP inhibited formation of the SCN plastic phase and additional silica nanoparticles were required to solidify the electrolyte for achieving a reported 3.81 % efficiency in solid state [37] (Jsc = 8.51 mA/cm<sup>2</sup>, Voc = 633 mV, FF = 71).

### ***3.2 Succinonitrile electrolyte with additives***

In an effort to compare the E1 liquid electrolyte containing BMII, I<sub>2</sub>, GSCN and TBP with a similar SCN based solid electrolyte, the effects of various additives on the performance of the BMII:I<sub>2</sub>:SCN solid were compared. Additives frequently employed in liquid electrolytes to improve the different aspects of DSSC performance are LiI, GSCN, TBP and NMBI. Their effects are summarized in Table 3 [34]. For this set of testing, a 6+0 working electrode configuration was employed. Additives were added to the BMII:I<sub>2</sub>:SCN electrolyte with stirring at 80°C to yield a molar ratio of 5:1:5:100 (BMII:I<sub>2</sub>:Additive:SCN).

All additives inhibited formation of the plastic phase of SCN by reducing its melting point and forming room temperature liquids in all cases except for the BMII:I<sub>2</sub>:GSCN:SCN combination, which remains as a solid at room temperature (Table 4). It is known that the melting point of

SCN is lowered by the addition of salts [21] and hence the results here are not surprising. A very low residual energy is required for the plastic-crystal phase to enter a more disordered state. Vacancies could account for several percent of the SCN's volume, but as the concentration of solutes increase, a tendency towards a partial loss of plastic-crystal local order occurs and eventually results in a complete inhibition of the plastic phase formation itself [21]. Decreased melting temperatures are noted with TBP, NMBI and LiI, which resulted in room temperature liquid formation. The addition of GSCN also exhibits a lowering of melting point as expected, but it still yields a room temperature solid. To the best of our knowledge, this is the first SCN based electrolyte to remain solid upon the addition of an extra additive. Succinonitrile consists of two  $\text{CH}_2\text{CN}$  moieties both involving a C triple bonded to N connected by a central C-C bond  $[\text{NCCH}_2\text{-CH}_2\text{CN}]$ . When additives are added to the system, a tendency towards inhibition of the plastic phase is observed due to the disordering of the SCN molecules in the plastic phase. The thiocyanate anion exhibits structural similarities to the succinonitrile molecule, containing a C triple bonded to N. It is possible that the nitrogen lone pair of the thiocyanate anion is interacting with the SCN host molecules, inducing some stabilization of the crystal order, and thereby comprising a slightly higher melting temperature than the other additive materials.

The additives TBP and NMBI performed as expected, increasing the cell voltage from 682 mV to 747 mV and 718 mV, respectively as displayed in Table 4 and Figure 3a. However this increase in voltage is associated with a decrease in cell current to  $J_{sc}$  values of  $9.09 \text{ mA/cm}^2$  and  $8.28 \text{ mA/cm}^2$ , respectively. Of these two additives, TBP performed better, which results in a higher  $V_{oc}$  and  $J_{sc}$ . Although  $V_{oc}$  is increased in both cases, due to the decrease in cell current a drop in overall efficiencies is observed from 4.84 % (no additive) to 4.35 % (TBP) and 3.57 % (NMBI).

The LiI additive yielded a remarkable increase in photocurrent. A  $J_{sc}$  value of  $16.0 \text{ mA/cm}^2$  was observed, much greater than the BMII analogue with no additives. This large current increase can be due to lithium cations being co-adsorbed onto  $\text{TiO}_2$  surface, which increases electron injection yield and thereby the cell current. However, a low voltage of 536 mV is observed. Coupled with a poor fill factor, a decrease in overall cell performance is noticed with an energy conversion efficiency of 3.75 %. Li ions can cause a positive shift of  $\text{TiO}_2$  conduction band, decreasing  $V_{oc}$  [31]. Also, the small Li ions can intercalate into the dye sensitised  $\text{TiO}_2$  films increasing recombination also lowering  $V_{oc}$ . Furthermore, the presence of  $\Gamma^-$  in the LiI additive can change the concentration of  $\Gamma^-/\text{I}_2$  in the electrolyte (compared to non-iodide containing TBP, NMBI and GSCN additives). This can change the poly-iodide distribution in the cell and alter the redox potential leading to higher or lower  $V_{oc}$  values. IPCE spectra were measured and it did not show any significant change in the iodide absorption spectral region (ESI Figure S2) but this effect cannot be ruled out entirely and it likely also affects the  $V_{oc}$ . In any case, the LiI addition showed poor cell performance as it resulted in a room temperature liquid due to inhibition of the SCN plastic phase formation. So, it was not pursued any further.

The GSCN additive resulted in a room temperature solid (Table 4). To the best of our knowledge, this is the first SCN/additive combination reported to form a room temperature solid without any additional solidifiers. The guanidinium cations act much like the lithium cation in that they are co-adsorbed onto  $\text{TiO}_2$  surface and increase the electron injection yield. Furthermore, guanidinium cations co-adsorbed onto the  $\text{TiO}_2$  surface alongside the dye anions allow for screening of the lateral Coulombic repulsion of the sensitiser [38]. As a result, a compact dye monolayer can be formed without molecular aggregation and the dark current systematically reduced. This causes a considerable increase in the open circuit voltage.

Consequently, compared to the non-additive BMII analogue an increase in Voc from 682 to 758 mV is observed. Unlike TBP and NMBI, there is no associated decrease in current. The trend of decreasing photocurrent as one progress from LiI to GSCN to TBP to NMBI additives (Table 4) is in agreement with the measured IPCE spectra (ESI Figure S2). The magnitude of IPCE is significantly lower for the TBP and NMBI additives, which is in agreement with their observed lower photocurrents. Although exhibiting a poor fill factor of 54 % with GSCN additive cell efficiency increases considerably from 4.84 % to 5.22 %..

The best combination of additive (GSCN) with BMII doped SCN was tested using our best 7+2 working electrode. Compared to the BMII:I<sub>2</sub>:SCN electrolyte with no additive, cell Voc improves considerably from 729 mV to 804 mV and is now comparable to that achieved with the liquid electrolyte (815 mV) as displayed in Table 5 and Figure 3b. There is no associated decrease in short circuit current density, either. However, the 15.5 mA/cm<sup>2</sup> J<sub>sc</sub> is still lower than that of the liquid electrolyte (18.1 mA/cm<sup>2</sup>). GSCN produces promising photocurrents and photovoltages, although the poor fill factor (48 %) translates them into a lower efficiency of 5.94 %. The low FF may be inherent to this solid electrolyte and could be related to poor pore filling of the thicker (15 micron) TiO<sub>2</sub> electrode. Improvements of this parameter would increase cell performance considerably. For example, with a relatively conservative FF of 58 % and the present Voc and Jsc values (804 mV, 15.5 mA/cm<sup>2</sup>) a remarkable efficiency of 7.2 % would be expected. Greater pore infiltration can be achieved by fluorine plasma treatment of the TiO<sub>2</sub> electrode [10], which increases the size of nanopores in the TiO<sub>2</sub> electrode however this would involve an additional fabrication step and was not pursued here.

Finally, of utmost interest is the cell durability/stability results of these electrolytes. Due to the low melting point of the SCN solid host (mp = 58 °C) they are expected to be most suitable for

indoor DSSC applications (Section 3.4). In this regard, we present the long term stability of the best performing cells after a period of 122 days stored in indoor, ambient, room temperature conditions in the dark (ESI Figure S3). 16 days after cell fabrication, the cells containing BMII:I<sub>2</sub>:SCN, DMPII:I<sub>2</sub>:SCN, BMII:I<sub>2</sub>:GSCN:SCN and E1 electrolytes show performances of 95%, 88%, 81% and 93%, respectively, compared to their maximum efficiency values. BMII:I<sub>2</sub>:SCN indeed exhibits quite a promising performance. The liquid E1 cell shows 79 % of its maximum performance after 122 days and the BMII:I<sub>2</sub>:SCN solid electrolyte maintains a promising 88%. Both the DMPII:I<sub>2</sub>:SCN and BMII:I<sub>2</sub>:GSCN:SCN electrolytes continue to exhibit the poor stability, which was observed already within the initial 16 days itself, now showing only 56% (DMPII:I<sub>2</sub>:SCN) and 43% (BMII:I<sub>2</sub>:GSCN:SCN) after 122 days.

### ***3.3 Manufacturing advantages***

The design of modules and integration of processing steps is critical to achieving high throughput and low cost DSSC production. Procedures such as electrolyte filling that are time consuming at the cell level must be done rapidly and efficiently when producing DSSC modules at commercial scales [28]. SCN based solid electrolytes offer several advantages in terms of DSSC manufacturing processes. Currently liquid phase electrolytes are introduced into the DSSC via a vacuum back filling process performed after cell sealing which involves several steps including:

- drilling hole in counter electrode (before cell fabrication)
- sandwich seal counter electrode and working electrode together
- vacuum back fill electrolyte
- seal back hole in counter electrode

Based on this study, we propose these steps can be reduced to one quick manufacturing line process suitable for rapid, low-cost, high-throughput continuous processing as outlined in Figure 4. A small bead of solid SCN electrolyte is dropped onto the dye coated TiO<sub>2</sub> at ambient temperature. The counter electrode is then brought towards the working electrode, sandwiching sealant material between the two electrodes. The cell is heated in order to cure the sealant material thereby sealing the cell. (Sealants currently employed in DSSC manufacturing line production generally involve curing conditions of UV irradiation with gentle heating at temperatures up to 80°C. This temperature range is perfect for use with low melting point SCN electrolyte and is amenable to the requirement that high temperature processing is avoided after dyeing as dye molecules are sensitive to temperature above 100°C [28]). Simultaneously the SCN electrolyte will begin to melt and slowly intercalate into the pores of the TiO<sub>2</sub> layer. The cell is then allowed to cool gradually to room temperature resulting in a sealed DSSC cell that is electrolyte filled and ready for use without the need for any tricky and time consuming vacuum electrolyte filling and back hole drilling and sealing steps. This procedure makes SCN very suitable for use in low-cost, high-throughput, continuous processing either in roll-to-roll manufacture on flexible materials or on rigid glass substrates.

### ***3.4 Low light (200 lx) measurement – indoor applications***

Finally, considering that the melting point of the SCN host is in the region of 60°C these electrolytes may be considered more suitable for use in indoor conditions where temperatures should not exceed 40°C. In this regard, the performance of the best cells was measured under low light conditions of a fluorescent bulb at an intensity of 200 Lx to simulate indoor lighting conditions as displayed in Table 6. The liquid electrolyte produced a maximum cell power of

2.65  $\mu\text{W}$ . Both the DMPII:I<sub>2</sub>:SCN and BMII:I<sub>2</sub>:SCN solids achieved less than half the performance of the liquid electrolyte. However BMII:I<sub>2</sub>:GSCN:SCN performed quite well achieving a power maximum of 1.63  $\mu\text{W}$  and exhibiting a much better FF under low light conditions compared to full sun (1000 W/m<sup>2</sup>) test conditions. Although not optimised, these results suggest that these solid electrolytes will perform under low light conditions and further optimisation of the electrolyte composition for use in low light (eg lower iodine/iodide concentrations) could yield promising potential for real world application of these SCN based materials.

#### **4. Conclusion**

Succinonitrile (SCN) doped with iodine and common imidazolium salts, DMPII and BMII, is possible to be used as a solid electrolyte in DSSC exhibiting best efficiencies of 6.3 % and 5.6 %, respectively. This result is achieved with a simple electrolyte filling process, without the use of any additives or additional TiO<sub>2</sub> electrode treatment.

The effect of common liquid electrolyte additives on their solid-state analogue of BMII:I<sub>2</sub>:SCN is now better understood. TBP and NMBI operate as expected, improving cell voltages, but reducing cell currents. LiI increases cell current, but causes considerable reduction in cell voltages and fill factor. GSCN improves cell Voc significantly with no drop in cell current. Cell performance can be improved from 5.6 % to 5.94 % when using the GSCN additive. Additives are found to inhibit formation of the SCN plastic phase. For the first time, a SCN/additive (GSCN) electrolyte composition is reported as a room temperature solid although its long term stability was found to be poor. The non-additive containing BMII:I<sub>2</sub>:SCN electrolyte shows most promising stability of the solid electrolytes tested.

The solid nature of the SCN host allows for easy processing in DSSC manufacturing lines. We outline a simple, ambient condition, single step procedure for DSSC electrolyte filling. Required manufacturing steps are reduced from four to one, allowing ready application of these solid electrolytes into DSSC manufacturing lines and enhancing DSSC's ability to compete with other PV technologies in terms of cost and manufacturing line speeds. Finally, these new electrolytes when tested under low light conditions at 200 Lx showed excellent promise for its use in DSSC meant for indoor and sensor applications.

### **Acknowledgements**

KRT acknowledges the SFI-Stokes Professorship grant support and award [S07/EN/E013].OB received support from European Commission's FP7 SMARTOP project under the Grant Agreement number: 265769. PKS acknowledges the funding support received from IRCSET and SolarPrint under the EMPOWER Industry partnership research funding programme. The authors would like to thank SolarPrint Ltd for 200 Lx measurements.

### **References:**

- 1 Wu, J., Lan, Z., Hao, S., Li, P., Lin, J., Huang, M., Fang, L., Huang, Y., Progress on the electrolytes for dye-sensitized solar cells. *Pure Appl. Chem.* 2008; **80**: 2241-2258, doi:10.1351/pac200880112241.
- 2 Chou, C.-S., Chou, F.-C., Kang, J.-Y., Preparation of ZnO-coated TiO<sub>2</sub> electrodes using dip coating and their applications in dye-sensitized solar cells. *Powder Technology* 2012; **215–216**: 38-45, doi:10.1016/j.powtec.2011.09.003.
- 3 Chiba, Y., Islam, A., Watanabe, Y., Komiya, R., Koide, N., Han, L., Dye-Sensitized Solar Cells with Conversion Efficiency of 11.1%. *Japanese Journal of Applied Physics* 2006; **45**: L638-L640, doi:10.1143/JJAP.45.L638.
- 4 Ito, S., Nazeeruddin, M. K., Liska, P., Comte, P., Charvet, R., Péchy, P., Jirousek, M., Kay, A., Zakeeruddin, S. M., Grätzel, M., Photovoltaic characterization of dye-sensitized solar cells: effect of device masking on conversion efficiency. *Progress in Photovoltaics: Research and Applications* 2006; **14**: 589-601, doi:10.1002/pip.683.
- 5 Yella, A., Lee, H.-W., Tsao, H. N., Yi, C., Chandiran, A. K., Nazeeruddin, M. K., Diau, E. W.-G., Yeh, C.-Y., Zakeeruddin, S. M., Grätzel, M., Porphyrin-Sensitized Solar Cells with Cobalt (II/III)-Based Redox Electrolyte Exceed 12 Percent Efficiency. *Science* 2011; **334**: 629-634, doi:10.1126/science.1209688.

- 6 Spiccia, L., Aqueous dye-sensitized solar cell electrolytes based on the cobalt(II)/(III) tris(bipyridine) redox couple. *Energy & Environmental Science* 2012, doi:10.1039/C2EE23317G.
- 7 Bai, Y., Cao, Y., Zhang, J., Wang, M., Li, R., Wang, P., Zakeeruddin, S. M. , Grätzel, M., High-performance dye-sensitized solar cells based on solvent-free electrolytes produced from eutectic melts. *Nat Mater* 2008; **7**: 626-630, doi:10.1038/nmat2224.
- 8 Chen, C.-L., Teng, H. , Lee, Y.-L., In Situ Gelation of Electrolytes for Highly Efficient Gel-State Dye-Sensitized Solar Cells. *Advanced Materials* 2011; **23**: 4199-4204, doi:10.1002/adma.201101448.
- 9 Wang, P., Zakeeruddin, S. M. , Grätzel, M., Solidifying liquid electrolytes with fluorine polymer and silica nanoparticles for quasi-solid dye-sensitized solar cells. *Journal of Fluorine Chemistry* 2004; **125**: 1241-1245, doi:10.1016/j.jfluchem.2004.05.010.
- 10 Lee, B., Buchholz, D. B., Guo, P., Hwang, D.-K. , Chang, R. P. H., Optimizing the Performance of a Plastic Dye-Sensitized Solar Cell. *The Journal of Physical Chemistry C* 2011; **115**: 9787-9796, doi:10.1021/jp201555n.
- 11 Chung, I., Lee, B., He, J., Chang, R. P. H. , Kanatzidis, M. G., All-solid-state dye-sensitized solar cells with high efficiency. *Nature* 2012; **485**: 486-489, doi:10.1038/nature11067.
- 12 Liu, X., Zhang, W., Uchida, S., Cai, L., Liu, B. , Ramakrishna, S., An Efficient Organic-Dye-Sensitized Solar Cell with in situ Polymerized Poly(3,4-ethylenedioxythiophene) as a Hole-Transporting Material. *Advanced Materials* 2010; **22**: E150-E155, doi:10.1002/adma.200904168.
- 13 Koh, J. K., Kim, J., Kim, B., Kim, J. H. , Kim, E., Highly Efficient, Iodine-Free Dye-Sensitized Solar Cells with Solid-State Synthesis of Conducting Polymers. *Advanced Materials* 2011; **23**: 1641-1646, doi:10.1002/adma.201004715.
- 14 Cai, N., Moon, S.-J., Cevey-Ha, L., Moehl, T., Humphry-Baker, R., Wang, P., Zakeeruddin, S. M. , Grätzel, M., An Organic D- $\pi$ -A Dye for Record Efficiency Solid-State Sensitized Heterojunction Solar Cells. *Nano Letters* 2011; **11**: 1452-1456, doi:10.1021/nl104034e.
- 15 Fabregat-Santiago, F., Bisquert, J., Cevey, L., Chen, P., Wang, M., Zakeeruddin, S. M. , Grätzel, M., Electron Transport and Recombination in Solid-State Dye Solar Cell with Spiro-OMeTAD as Hole Conductor. *Journal of the American Chemical Society* 2009; **131**: 558-562, doi:10.1021/ja805850q.
- 16 Kumara, G. R. A., Okuya, M., Murakami, K., Kaneko, S., Jayaweera, V. V. , Tennakone, K., Dye-sensitized solid-state solar cells made from magnesiumoxide-coated nanocrystalline titanium dioxide films: enhancement of the efficiency. *Journal of Photochemistry and Photobiology A: Chemistry* 2004; **164**: 183-185, doi:10.1016/j.jphotochem.2003.11.020.
- 17 Burschka, J., Pellet, N., Moon, S.-J., Humphry-Baker, R., Gao, P., Nazeeruddin, M. K. , Grätzel, M., Sequential deposition as a route to high-performance perovskite-sensitized solar cells. *Nature* 2013; **499**: 316-319, doi:10.1038/nature12340.
- 18 Dai, Q., MacFarlane, D. R. , Forsyth, M., High mobility  $I^-/I_3^-$  redox couple in a molecular plastic crystal: A potential new generation of electrolyte for solid-state photoelectrochemical cells. *Solid State Ionics* 2006; **177**: 395-401, doi:10.1016/j.ssi.2005.11.004.
- 19 Hawthorne, H. M. , Sherwood, J. N., Lattice defects in plastic organic solids. Part 2.-Anomalous self-diffusion in succinonitrile. *Transactions of the Faraday Society* 1970; **66**: 1792-1798, doi:10.1039/TF9706601792.
- 20 MacFarlane, D. R., Huang, J. , Forsyth, M., Lithium-doped plastic crystal electrolytes exhibiting fast ion conduction for secondary batteries. *Nature* 1999; **402**: 792-794, doi:10.1038/45514.
- 21 Alarco, P.-J., Abu-Lebdeh, Y., Abouimrane, A. , Armand, M., The plastic-crystalline phase of succinonitrile as a universal matrix for solid-state ionic conductors. *Nat Mater* 2004; **3**: 476-481, doi:10.1038/nmat1158.
- 22 Long, S., MacFarlane, D. R. , Forsyth, M., Fast ion conduction in molecular plastic crystals. *Solid State Ionics* 2003; **161**: 105, doi:10.1016/S0167-2738(03)00208-X.

- 23 Abu-Lebdeh, Y., Abouimrane, A., Alarco, P. J., Hammami, A., Ionescu-Vasii, L. , Armand, M., Ambient temperature proton conducting plastic crystal electrolytes. *Electrochem. Commun.* 2004; **6**: 432, doi:10.1016/j.elecom.2004.02.015.
- 24 Wang, P., Dai, Q., Zakeeruddin, S. M., Forsyth, M., MacFarlane, D. R. , Grätzel, M., Ambient Temperature Plastic Crystal Electrolyte for Efficient, All-Solid-State Dye-Sensitized Solar Cell. *Journal of the American Chemical Society* 2004; **126**: 13590-13591, doi:10.1021/ja045013h.
- 25 Hwang, D., Jo, S. M., Kim, D. Y., Armel, V., MacFarlane, D. R. , Jang, S.-Y., High-Efficiency, Solid-State, Dye-Sensitized Solar Cells Using Hierarchically Structured TiO<sub>2</sub> Nanofibers. *ACS Applied Materials & Interfaces* 2011; **3**: 1521-1527, doi:10.1021/am200092j.
- 26 Desilvestro, H., Beretz, M., Tulloch, S. , Tulloch, G. E. in *Dye Sensitised Solar Cells* (ed K. Kalyanasundaram) Ch. 7, 'Packaging, Scale-up, and Commercialization of Dye Solar Cells', (EPFL Press, 2010).
- 27 Pettersson, H., Nonomura, K., Kloo, L. , Hagfeldt, A., Trends in patent applications for dye-sensitized solar cells. *Energy & Environmental Science* 2012; **5**: 7376-7380.
- 28 Baxter, J. B., Commercialization of dye sensitized solar cells: Present status and future research needs to improve efficiency, stability, and manufacturing. *Journal of Vacuum Science & Technology A: Vacuum, Surfaces, and Films* 2012; **30**: 020801, doi:10.1116/1.3676433.
- 29 Hinsch, A., Brandt, H., Veurman, W., Hemming, S., Nittel, M., Würfel, U., Putyra, P., Lang-Koetz, C., Stabe, M., Beucker, S. , Fichter, K., Dye solar modules for facade applications: Recent results from project ColorSol. *Solar Energy Materials and Solar Cells* 2009; **93**: 820-824, doi:<http://dx.doi.org/10.1016/j.solmat.2008.09.049>.
- 30 Hinsch, A., Veurman, W., Brandt, H., Loayza Aguirre, R., Bialecka, K. , Flarup Jensen, K., Worldwide first fully up-scaled fabrication of 60 × 100 cm<sup>2</sup> dye solar module prototypes. *Progress in Photovoltaics: Research and Applications* 2012; **20**: 698-710, doi:10.1002/pip.1213.
- 31 Kroon, J. M., Bakker, N. J., Smit, H. J. P., Liska, P., Thampi, K. R., Wang, P., Zakeeruddin, S. M., Grätzel, M., Hinsch, A., Hore, S., Würfel, U., Sastrawan, R., Durrant, J. R., Palomares, E., Pettersson, H., Gruszecki, T., Walter, J., Skupien, K. , Tulloch, G. E., Nanocrystalline dye-sensitized solar cells having maximum performance. *Progress in Photovoltaics: Research and Applications* 2007; **15**: 1-18, doi:10.1002/pip.707.
- 32 Ito, S., Murakami, T. N., Comte, P., Liska, P., Grätzel, C., Nazeeruddin, M. K. , Grätzel, M., Fabrication of thin film dye sensitized solar cells with solar to electric power conversion efficiency over 10%. *Thin Solid Films* 2008; **516**: 4613-4619, doi:10.1016/j.tsf.2007.05.090.
- 33 Ito, S., Chen, P., Comte, P., Nazeeruddin, M. K., Liska, P., Péchy, P. , Grätzel, M., Fabrication of screen-printing pastes from TiO<sub>2</sub> powders for dye-sensitised solar cells. *Progress in Photovoltaics: Research and Applications* 2007; **15**: 603-612, doi:10.1002/pip.768.
- 34 Yu, Z., Vlachopoulos, N., Gorlov, M. , Kloo, L., Liquid electrolytes for dye-sensitized solar cells. *Dalton Transactions* 2011; **40**: 10289-10303, doi:10.1039/C1DT11023C.
- 35 Sapp, S. A., Elliott, C. M., Contado, C., Caramori, S. , Bignozzi, C. A., Substituted Polypyridine Complexes of Cobalt(II/III) as Efficient Electron-Transfer Mediators in Dye-Sensitized Solar Cells. *Journal of the American Chemical Society* 2002; **124**: 11215-11222, doi:10.1021/ja027355y.
- 36 Liu, Y., Hagfeldt, A., Xiao, X.-R. , Lindquist, S.-E., Investigation of influence of redox species on the interfacial energetics of a dye-sensitized nanoporous TiO<sub>2</sub> solar cell. *Solar Energy Materials and Solar Cells* 1998; **55**: 267-281, doi:10.1016/s0927-0248(98)00111-1.
- 37 Li, D., Qin, D., Deng, M., Luo, Y. , Meng, Q., Optimization the solid-state electrolytes for dye-sensitized solar cells. *Energy & Environmental Science* 2009; **2**: 283-291, doi:10.1039/B813378F.
- 38 Grätzel, M., Conversion of sunlight to electric power by nanocrystalline dye-sensitized solar cells. *Journal of Photochemistry and Photobiology A: Chemistry* 2004; **164**: 3-14, doi:10.1016/j.jphotochem.2004.02.023.

**Table 1.** Some of the best DSSC performances reported for cells containing liquid, solid and quasi-solid phase electrolytes\*

Electrolyte		Sensitiser	$\eta$ (%)	Voc (mV)	Jsc (mA/cm <sup>2</sup> )	FF	ref
Liquid	AY1:[Co <sup>II</sup> (bpy) <sub>3</sub> ](B(CN) <sub>4</sub> ) <sub>2</sub> (0.165 M), [Co <sup>III</sup> (bpy) <sub>3</sub> ](B(CN) <sub>4</sub> ) <sub>3</sub> (0.045M), TBP (0.8M), LiClO <sub>4</sub> (0.1M) in ACN solvent	YD2- <i>o</i> -C8+Y123	12.3	935	17.66	74	[5]
	DMPII (0.6 M), LiI (0.1 M), I <sub>2</sub> (0.05 M), TBP (0.5 M) in ACN	Black dye	11.1	736	20.9	72.2	[3]
	E1: BMII (0.6 M), I <sub>2</sub> (0.03 M), GSCN (0.1 M), TBP (0.5 M) in ACN:valeronitrile (vol ratio: 85:15)) - [no mask]	N719	9.82 12.2	820 832	16.0 20.1	74.5 73.1	[4]
	Solvent Free: DMII/EMII/EMITCB/I <sub>2</sub> /NBB/GSCN (Molar ratio: 12;12;16;1.67;3.33;0.67)	Z907Na	8.2	741	14.26	77.4	[7]
Gel/quasi-solid	LiI (0.1 M), I <sub>2</sub> (0.05 M), TBP (0.5 M), DMPII (0.5 M) in ACN + Poly(acrylonitrile- <i>co</i> -vinyl acetate) (PAN-VA)	N719	9.03	797	15.44	73	[8]
	LiI (0.1 M), I <sub>2</sub> (0.05 M), TBP (0.5 M), DMPII (0.5 M) in ACN + (PAN-VA) + TiO <sub>2</sub> filler (10 wt%)	N719	9.46	794	16.23	73	[8]
	PMII (0.6 M), I <sub>2</sub> (0.1 M), NMBI (0.45 M) in MPN + PVDF-HFP (5 wt%)	Z907	6.7	749	13.1	68.1	[9]
Solid	spiro-MeOTAD doped with Co(III) complex	CH <sub>3</sub> NH <sub>3</sub> PbI <sub>3</sub>	15.0	993	20.0	73	[17]
	P <sub>1,4</sub> I <sub>2</sub> /Succinonitrile (5:1:100) (Plasma treated TiO <sub>2</sub> electrode, two step filling procedure)	N719	9.37	763	17.1	71.4	[10]
	CsSnI <sub>2.95</sub> F <sub>0.05</sub> doped with 5% SnF <sub>2</sub> (Plasma treated TiO <sub>2</sub> electrode)	N719	9.28	730	17.4	72.9	[11]
	PEDOT + Li salt/propylene carbonate solution	D149	6.1	860	9.3	75	[12]
	PEDOT doped with LiTFSI, MPII, TBP	N719	5.4	640	14.2	60	[13]
	Spiro-MeOTAD (0.17 M), TBP (0.11 mM), LiN(CF <sub>3</sub> SO <sub>2</sub> ) <sub>2</sub> (0.21 mM) in chlorobenzene	C220	6.08	860	10.90	69	[14]
	Spiro-OMeTAD	Z907	4	860	9.1	51	[15]
	CuI (MgO coated TiO <sub>2</sub> electrode)	N3	4.7	620	13.0	58	[16]

\*See text and references for explanation of abbreviations.

**Table 2.** Photovoltaic parameters of DSSC devices made with the listed electrolytes at 1 sun ( $1000 \text{ Wm}^{-2}$ ) incident intensity of AM1.5 simulated solar light.

Electrolyte	Jsc ( $\text{mA/cm}^2$ )	Voc (V)	FF	$\eta$ (%)
Liquid (E1)	18.1	0.815	57	8.47
<i>DMPII</i> : $I_2$ :SCN	15.6	0.707	57	6.33
<i>BMII</i> : $I_2$ :SCN	13.4	0.729	58	5.62
<i>LiI</i> : $I_2$ :SCN	14.6	0.489	50	3.58

\* electrolyte compositions: E1 is liquid phase and composed of 0.03M iodine, 0.1M guanidinium thiocyanate, 0.5M 4-*tert*-butylpyridine and 0.6M BMII in acetonitrile:valeronitrile solution (85:15 by volume). Solid state electrolytes consist of: DMPII, BMII or LiI dispersed with iodine ( $I_2$ ) in SCN in the molar ratio 5:1:100 (X- $I_2$ :SCN).

**Table 3.** Summary of the effects of different electrolyte additives on DSSC cell performance[34]

Additive	Lithium Iodide (LiI)	Guanidinium Thiocyanate (GSCN)	4-tert-butylpyridine (TBP) and N-methylbenz-imidazole (NMBI)
Effect	Increase Isc Reduce Voc	Increase Isc Increase Voc	Increase Voc
Comment	<p>Li<sup>+</sup> adsorbed onto TiO<sub>2</sub> surface: → increase electron injection yield (increase current)</p> <p>→ Positive shift of TiO<sub>2</sub> conduction band (decrease Voc)</p> <p>Li ions intercalate into dye sensitized TiO<sub>2</sub> films → increase recombination (decrease Voc)</p>	<p>Guanidinium cations adsorbed onto TiO<sub>2</sub> surface: → increase electron injection yield (increase current)</p> <p>→ self assembly of compact dye layer - slower electron recombination rate (increase Voc)</p>	<p>Negative shift of TiO<sub>2</sub> conduction band: → increase Voc</p> <p>Longer electron lifetimes in CB → slower electron recombination rate (increase Voc)</p>

**Table 4.** Photovoltaic parameters of DSSC devices made with BMII:I<sub>2</sub>:SCN electrolyte and our 6+0 working electrode configuration with different additives at 1 sun (1000 Wm<sup>-2</sup>) incident intensity of AM1.5 simulated solar light. Their phase at room temperature and 10°C is also listed.

Electrolyte	J <sub>sc</sub> (mA/cm <sup>2</sup> )	V <sub>oc</sub> (V)	FF	η(%)	Phase at room temp.	Phase at 10°C
Liquid (E1)	11.8	0.720	72	6.24	Liquid	Liquid
<i>BMII:I<sub>2</sub>:SCN</i>	12.2	0.682	58	4.84	Solid	Solid
<i>BMII:I<sub>2</sub>:<u>LiI</u>:SCN</i>	16.0	0.536	44	3.75	Liquid	Solid
<i>BMII:I<sub>2</sub>:<u>GSCN</u>:SCN</i>	12.8	0.758	54	5.22	Solid	Solid
<i>BMII:I<sub>2</sub>:<u>TBP</u>:SCN</i>	9.09	0.747	64	4.35	Liquid	Solid
<i>BMII:I<sub>2</sub>:<u>NMBI</u>:SCN</i>	8.28	0.718	60	3.57	Liquid	Solid

\* electrolyte compositions: E1 is liquid phase and composed of 0.03M iodine, 0.1M guanidinium thiocyanate, 0.5M 4-*tert*-butylpyridine and 0.6M BMII in acetonitrile:valeronitrile solution (85:15 by volume). Succinonitrile based electrolytes consist of: BMII dispersed with iodine (I<sub>2</sub>) in SCN with the listed additive (LiI, GSCN, TBP or NMBI) in the molar ratio 5:1:5:100 (BMII:I<sub>2</sub>:Additive:SCN).

**Table 5.** Photovoltaic parameters of the devices made with BMII:I<sub>2</sub> electrolyte with different additives and/or solvents and our best 7+2 working electrode configuration at 1 sun (1000 Wm<sup>-2</sup>) incident intensity of AM1.5 simulated solar light.

Electrolyte	J <sub>sc</sub> (mA/cm <sup>2</sup> )	V <sub>oc</sub> (V)	FF	η <sub>1</sub> (%)
Liquid (E1) (BMII:I <sub>2</sub> :GSCN:TBP)	18.1	0.815	57	8.47
Solid (BMII:I <sub>2</sub> :GSCN:SCN)	15.5	0.804	48	5.94
Solid (BMII:I <sub>2</sub> :SCN)	13.4	0.729	58	5.62

\* electrolyte compositions: E1 is liquid phase and composed of 0.03M iodine, 0.1M guanidinium thiocyanate, 0.5M 4-*tert*-butylpyridine and 0.6M BMII in acetonitrile:valeronitrile solution (85:15 by volume). Succinonitrile based electrolytes consist of: BMII dispersed with iodine (I<sub>2</sub>) in SCN in the molar ratio 5:1:100 (BMII:I<sub>2</sub>:SCN) and with GSCN additive in the molar ratio 5:1:5:100 (BMII:I<sub>2</sub>:GSCN:SCN).

**Table 6.** Photovoltaic parameters of DSSC devices made with different electrolyte materials at 200 Lx incident intensity of fluorescent light.

Electrolyte	Jsc ( $\mu\text{A}/\text{cm}^2$ )	Voc (V)	FF (%)	Pmax ( $\mu\text{W}$ )
Liquid (E1)	23.7	0.654	61	2.65
<b>DMPII:I<sub>2</sub>:SCN</b>	16.5	0.379	48	0.85
<b>BMII:I<sub>2</sub>:SCN</b>	17.2	0.419	50	1.01
<b>BMII:I<sub>2</sub>:GSCN:SCN</b>	16.6	0.542	65	1.63

\* electrolyte compositions: E1 is liquid phase and composed of 0.03M iodine, 0.1M guanidinium thiocyanate, 0.5M 4-*tert*-butylpyridine and 0.6M BMII in acetonitrile:valeronitrile solution (85:15 by volume). Succinonitrile based electrolytes consist of: DMPII dispersed with iodine (I<sub>2</sub>) in SCN in the molar ratio 5:1:100 (DMPII:I<sub>2</sub>:SCN), BMII dispersed with iodine (I<sub>2</sub>) in SCN in the molar ratio 5:1:100 (BMII:I<sub>2</sub>:SCN) and with GSCN additive in the molar ratio 5:1:5:100 (BMII:I<sub>2</sub>:GSCN:SCN).

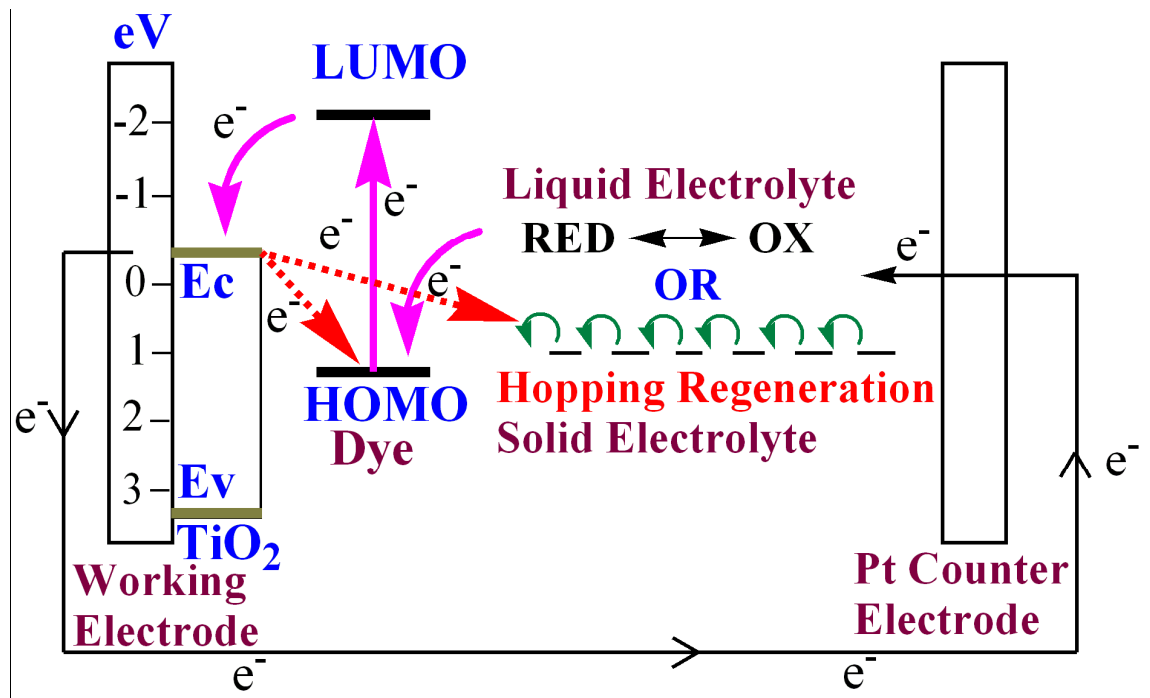


**Figure 1.** Operational outline of DSSC. Undesired recombination processes are displayed as red dashed arrows.

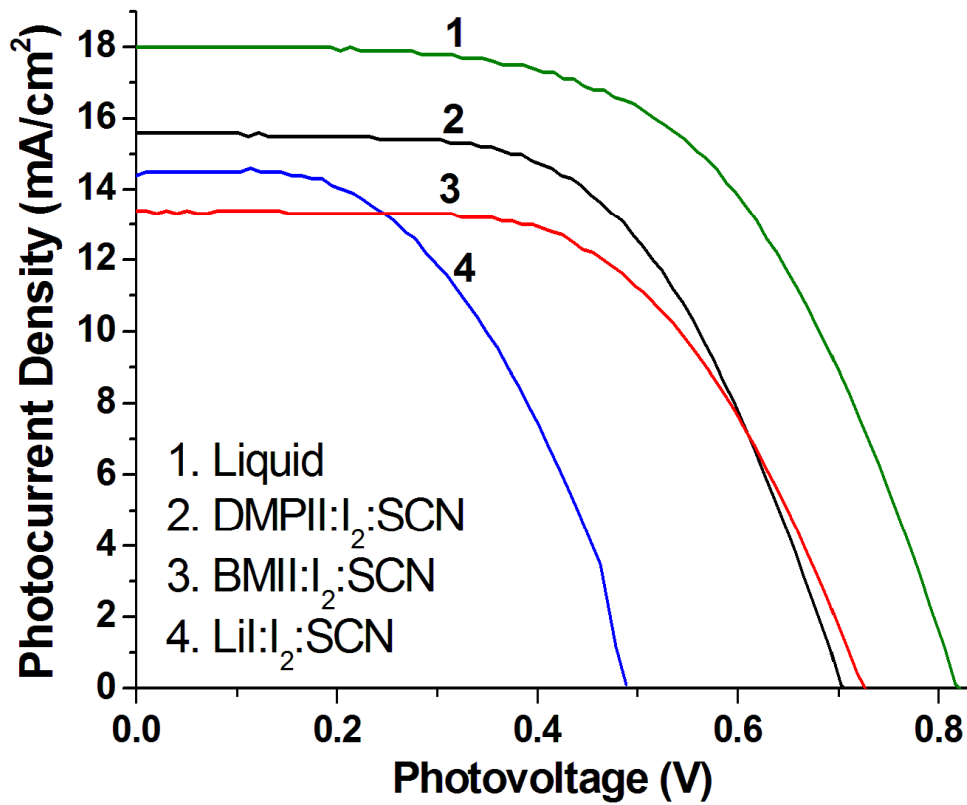


**Figure 2.** J-V curves for DSSC using different electrolyte materials measured under standard AM1.5 conditions.

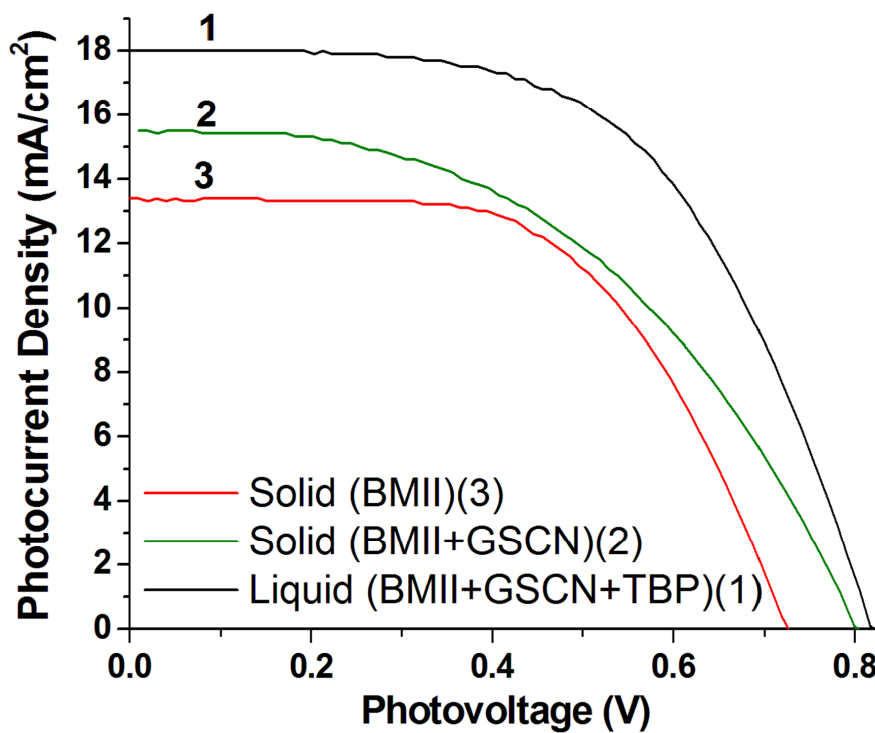
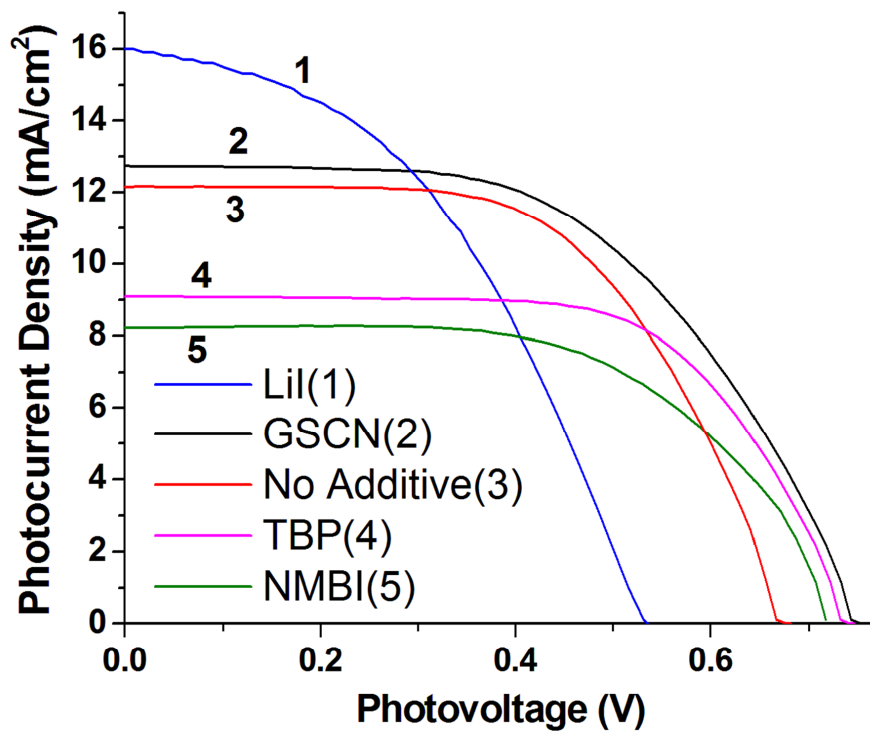


**Figure 3.** a) [top graphs] J-V curves for DSSC using BMII:I<sub>2</sub>:SCN electrolyte with different additives. b) [bottom graphs] J-V curves for DSSC using BMII:I<sub>2</sub> based electrolytes and our best TiO<sub>2</sub> electrode configuration.

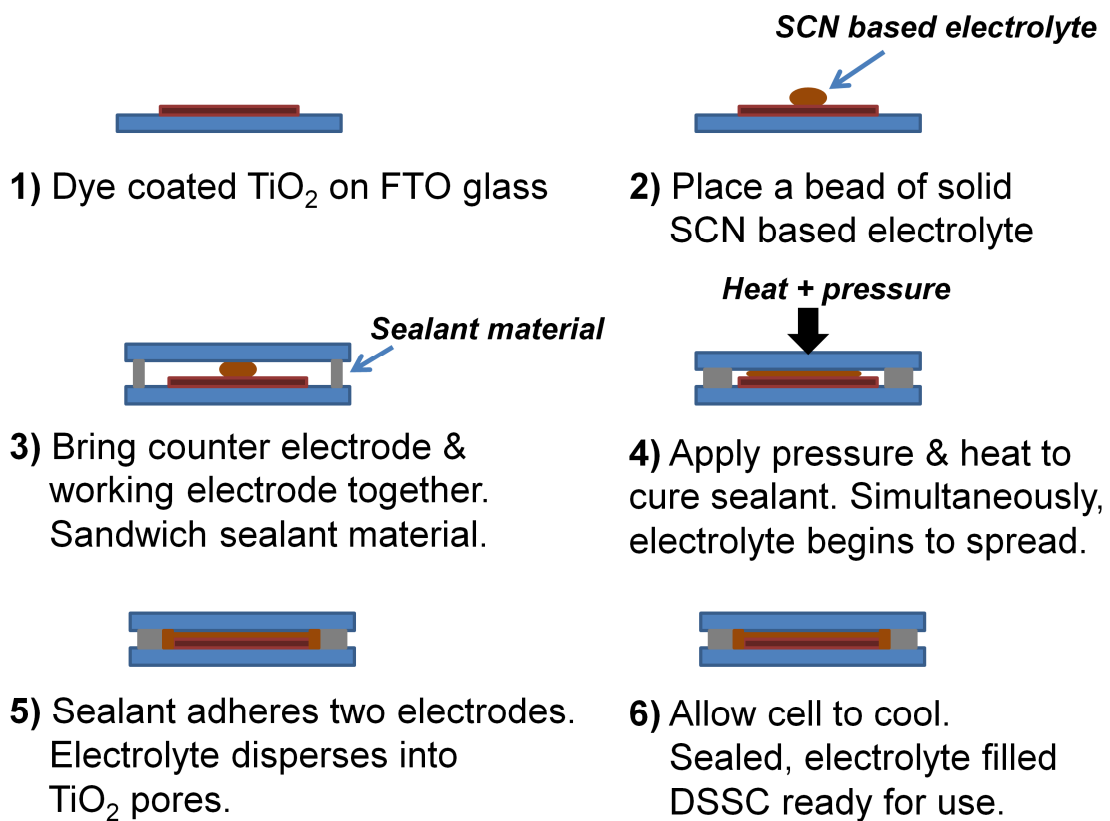


**Figure 4.** Electrolyte filling and DSSC cell sealing step using solid state SCN based electrolytes.

## Succinonitrile based solid state electrolytes for dye sensitised solar cells.

*Owen Byrne, Aoife Coughlan, Praveen K. Surolia, K. Ravindranathan Thampi\**

### Electronic Supporting Information (ESI):

**Table S1.** Average performance of multiple devices using the room temperature solid Succinonitrile (SCN) based electrolytes consisting of: DMPII dispersed with iodine (I<sub>2</sub>) in SCN in the molar ratio 5:1:100 (DMPII:I<sub>2</sub>:SCN), BMII dispersed with iodine (I<sub>2</sub>) in SCN in the molar ratio 5:1:100 (BMII:I<sub>2</sub>:SCN) and with GSCN additive in the molar ratio 5:1:5:100 (BMII:I<sub>2</sub>:GSCN:SCN) made with our best 7+2 working electrode configuration.

Electrolyte	Jsc (mA/cm <sup>2</sup> )	Voc (V)	FF	η (%)	Average η (%)	% deviation
<b>BMII:I<sub>2</sub>: SCN</b>	15.1	0.708	48	5.08	<b>5.33</b>	-4.6
	14.9	0.715	51	5.46		+2.5
	13.3	0.672	57	5.14		-3.5
	13.4	0.729	58	5.62		+5.5
<b>DMPII:I<sub>2</sub>:S CN</b>	15.6	0.707	57	6.33	<b>5.31</b>	+19.2
	13.4	0.743	52	5.17		-2.6
	11.4	0.704	60	4.81		-9.4
	12.6	0.680	58	4.93		-7.2
<b>BMII:I<sub>2</sub>: GSCN: SCN</b>	15.5	0.804	48	5.94	<b>5.04</b>	+17.9
	14.0	0.735	52	5.32		+5.7
	14.6	0.733	40	4.24		-15.8
	14.8	0.727	43	4.64		-7.8

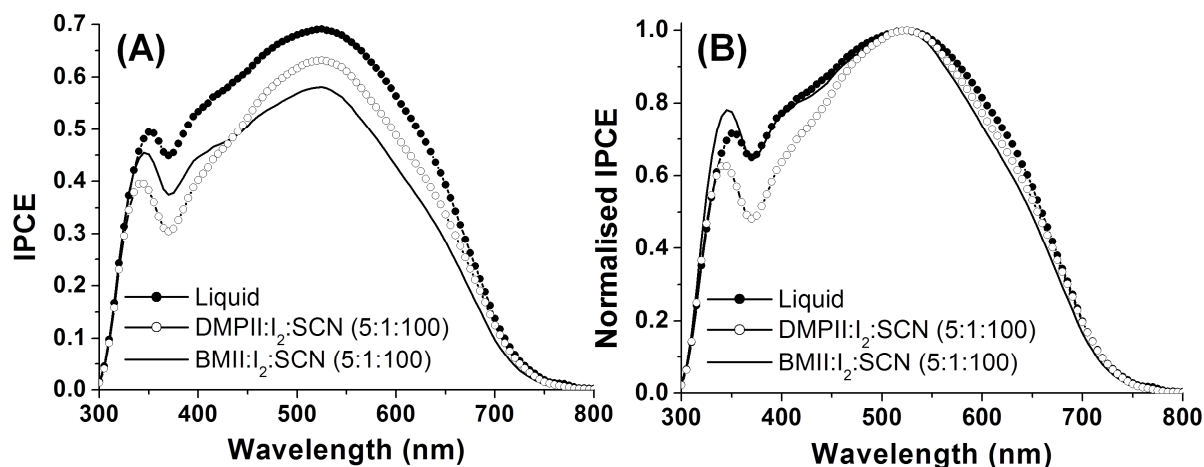


**Figure S1.** IPCE spectra of the solid state DMPII and BMII based SCN electrolytes compared to liquid E1 electrolyte. **(A)** Measured IPCE spectra. Maximum response of 69 % (E1), 58 % (BMII) and 63 % (DMPII) are observed at 525 nm. **(B)** Normalised IPCE spectra allowing comparison of spectral response. Solid state DMPII: $I_2$ :SCN shows slightly lesser IPCE response in the ~350-450 nm region compared to E1 and BMII: $I_2$ :SCN. [electrolyte compositions: E1 = 0.03M iodine, 0.1M guanidinium thiocyanate, 0.5M 4-tert-butylpyridine and 0.6M BMII in acetonitrile /valeronitrile solution (85:15 by volume). Solid state electrolytes consist of: DMPII or BMII dispersed with iodine ( $I_2$ ) in SCN in the molar ratio 5:1:100 (X- $I_2$ :SCN).]

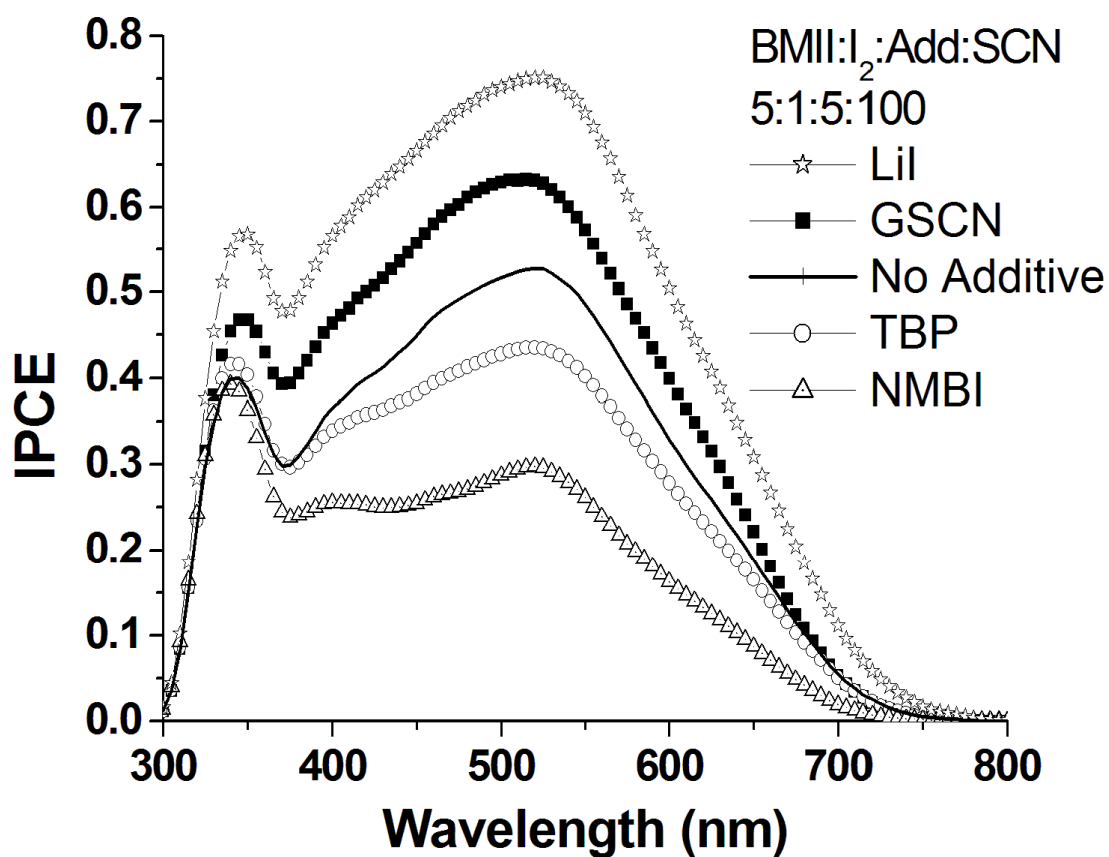


**Figure S2.** IPCE spectra of DSSC containing the BMII:I<sub>2</sub>:SCN electrolyte (solid line) and IPCE of the BMII:I<sub>2</sub>:SCN electrolyte containing various additives. Electrolyte consists of BMII dispersed with iodine (I<sub>2</sub>) in SCN in the molar ratio 5:1:100 (BMII:I<sub>2</sub>:SCN) or with the listed additive (LiI, GSCN, TBP or NMBI) in the molar ratio 5:1:5:100 (BMII:I<sub>2</sub>:Additive:SCN).

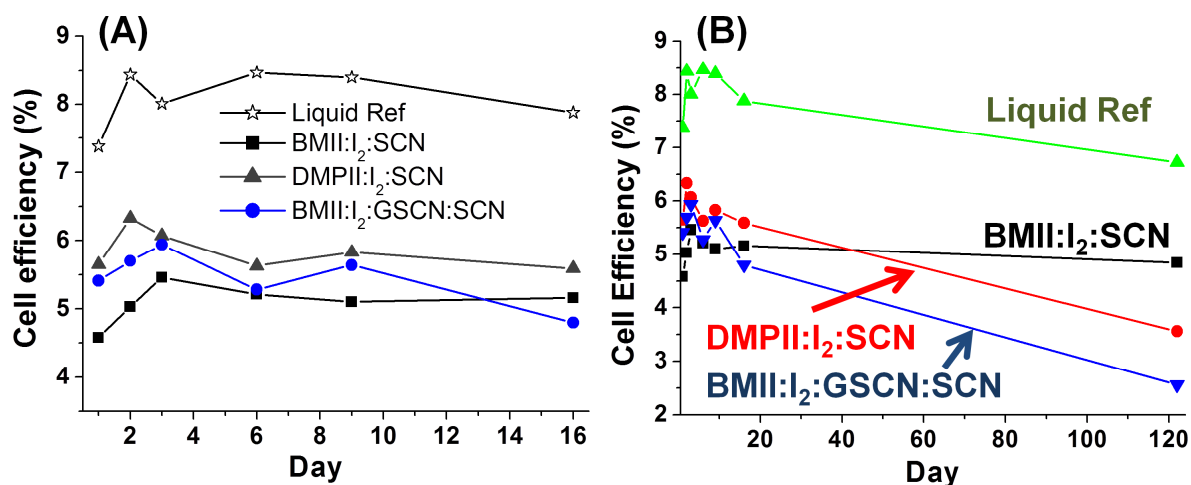


**Figure S3.** Stability testing of solid state SCN based electrolytes. The cells were stored for a period of up to 122 days in indoor, ambient, room temperature conditions in the dark. **A)** First 16 days after cell fabrication. Cells containing BMII:I<sub>2</sub>:SCN, DMPII:I<sub>2</sub>:SCN, BMII:I<sub>2</sub>:GSCN:SCN and E1 electrolytes show values of 95%, 88%, 81% and 93% respectively on Day 16 compared to their maximum performance. **B)** Cell stability after a period of 122 days. The liquid ref E1 cell exhibits 79 % of its maximum performance after this time and the BMII:I<sub>2</sub>:SCN solid electrolyte maintains a promising 88 %. The DMPII:I<sub>2</sub>:SCN and BMII:I<sub>2</sub>:GSCN:SCN electrolytes exhibit 56 % and 43 % respectively. [Electrolyte compositions: Liquid Ref, E1 = 0.03M iodine, 0.1M guanidinium thiocyanate, 0.5M 4-tert-butylpyridine and 0.6M BMII in acetonitrile /valeronitrile solution (85:15 by volume). Solid state electrolytes consist of: DMPII or BMII dispersed with iodine (I<sub>2</sub>) in SCN in the molar ratio 5:1:100 (X-I:I<sub>2</sub>:SCN) and BMII:I<sub>2</sub>:GSCN:SCN in the molar ratio 5:1:5:100.]